

Quantum phase transition in a single-molecule quantum dot

Nicolas Roch¹, Serge Florens¹, Vincent Bouchiat¹, Wolfgang Wernsdorfer¹ & Franck Balestro¹
¹*Institut Néel, Nanosciences Department, associé à l'UJF,
CNRS, BP 166, 38042 Grenoble Cedex 9, France*

Quantum criticality is the intriguing possibility offered by the laws of quantum mechanics when the wave function of a many-particle physical system is forced to evolve continuously between two distinct, competing ground states. This phenomenon, often related to a zero-temperature magnetic phase transition, can be observed in several strongly correlated materials such as heavy fermion compounds or possibly high-temperature superconductors, and is believed to govern many of their fascinating, yet still unexplained properties. In contrast to these bulk materials with very complex electronic structure, artificial nanoscale devices could offer a new and simpler vista to the comprehension of quantum phase transitions. This long-sought possibility is demonstrated by our work in a fullerene molecular junction, where gate voltage induces a crossing of singlet and triplet spin states at zero magnetic field. Electronic tunneling from metallic contacts into the C₆₀ quantum dot provides here the necessary many-body correlations to observe a true quantum critical behavior.

PACS numbers:

INTRODUCTION

In order to grasp the fundamental difference between classical and quantum phase transitions, one can start with the basic principle of thermodynamics that systems in thermal equilibrium lie in their minimal free energy state. As a consequence, a change in temperature can drive a classical phase transition by a competition between low energy configurations and the entropy associated to thermal fluctuations. However, strictly at zero temperature, most physical systems have quenched their entropy and some kind of order may be expected. Even then, Heisenberg's uncertainty principle of quantum mechanics implies that zero-point motion is always present. If the strength of these quantum fluctuations can be increased by changing some non-thermal parameter λ (in analogy to an increase of temperature), the ground state of the system may evolve between two wavefunctions with different symmetries, $|A\rangle$ and $|B\rangle$, by a quantum phase transition at a critical value $\lambda \approx \lambda_c$ (Fig. 1a). Interestingly, even if absolute zero temperature is experimentally unaccessible, quantum phase transitions leave peculiar fingerprints that are visible at non zero temperature [1].

Quantum Dots (QDs) seem then to be ideal devices to observe quantum phase transitions. First, such gate-tunable artificial atoms offer a high degree of control by simple gate electrostatics. Second, due to the nanometric confinement of the electrons, they display relatively high energy scales that allow the observation of interesting quantum phenomena at low temperature. Finally, the coupling between the QD and the electronic reservoirs (transport probes) provides tunneling events that can fundamentally alter the dot states into complicated many-body wavefunctions. One well studied situation (although not classified as a quantum transition) where these three points fortuitously play together occurs when a single unpaired spin $S = 1/2$ characterizes the ground

state of the QD. When conducting electrons move to-and-from the device while reversing the tiny magnetic moment of the dot, a progressive screening of the atomic spin occurs, in complete analogy to the well-known Kondo effect in solids containing magnetic impurities [2, 3]. The Kondo effect in QDs is then observed as zero-bias conductance resonance [4, 5], associated to the entangled state of electrons in the leads and in the dot, and which displays a high degree of universality.

QDs with even occupancy introduce the possibility of having a singlet or a triplet spin state, if the coupling to the electrodes may be neglected. When the Kondo effect sets in to meet the singlet-triplet splitting, a subtle competition occurs for the fate of the dot magnetic state, which was predicted to turn the singlet-triplet crossing into a true zero-temperature quantum phase transition, although different theoretical scenarios have been put forward, depending whether one [6, 7] or two [8, 9] screening channels are involved. While quantum critical phenomena related to Kondo screening have been attributed to the astonishing properties of many strongly correlated materials [10], a clear-cut observation in nanostructures of a screening-unscreening transition is still lacking. This is despite the intensive studies of singlet-triplet Kondo effects measured through vertical quantum dots [11], GaAs lateral quantum dots under an applied magnetic field [12, 13], or at zero magnetic field [14, 15], carbon nanotubes [16, 17, 18, 19], and double dot structures [20]. Indeed, the ability to observe a sharp quantum transition is limited either by the existence of two screening electronic channels (linked to conserved orbital quantum numbers), which generically give an avoided transition [21, 22], or by relatively low Kondo temperatures, leading to the broad features observed in those experiments.

C₆₀ QDs inserted in a nanoscale constriction present several key ingredients for observing a quantum phase

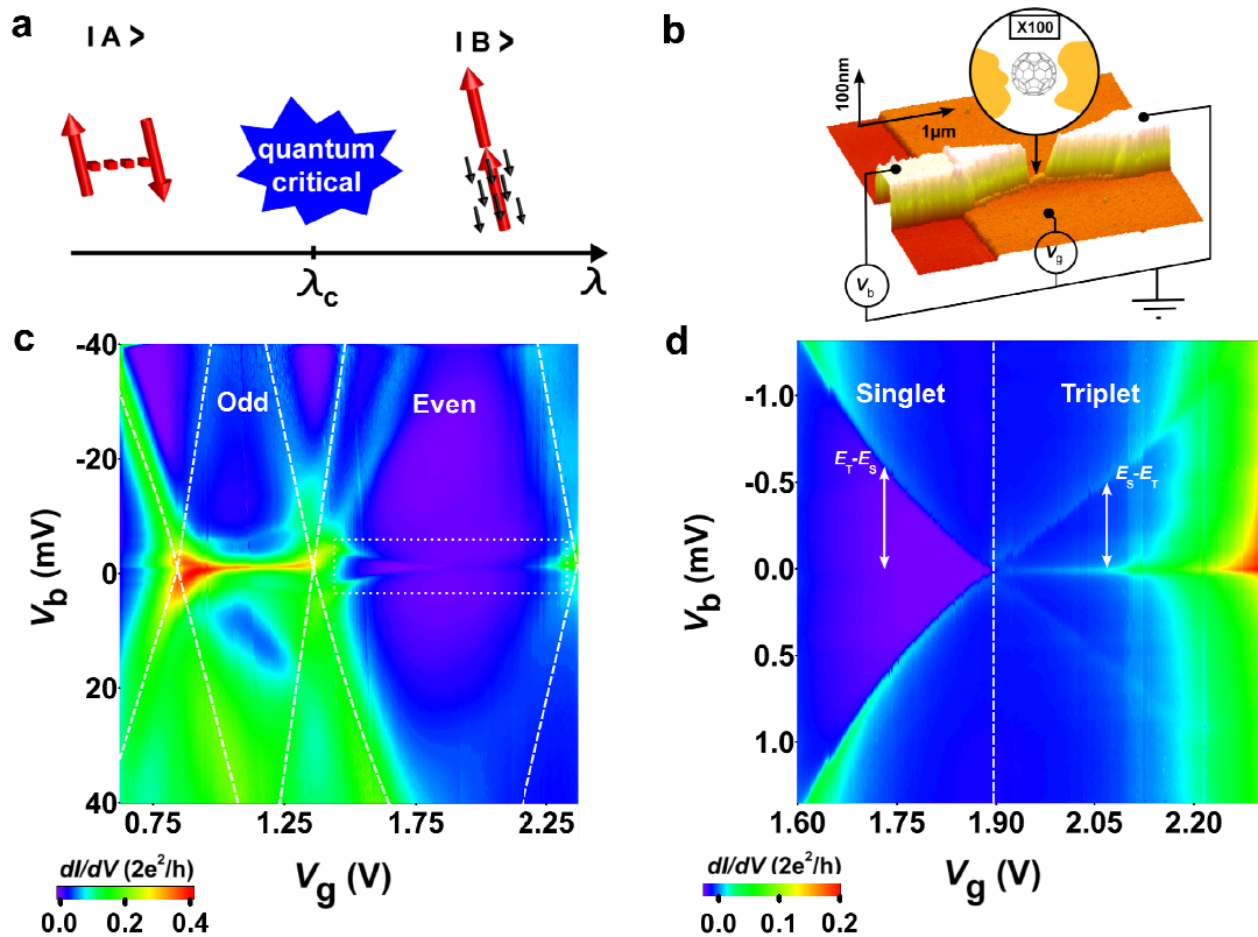


FIG. 1: **Quantum phase transition, device and device characteristics.** **a**, Quantum phase transition: a quantum state $|A\rangle$ can be driven by a non-thermal external parameter λ to another quantum state $|B\rangle$ with a different symmetry through a critical point at $\lambda = \lambda_c$. In our C_{60} QD device, $|A\rangle$ is a singlet, and $|B\rangle$ is a triplet, partially screened by one conduction electron channel represented by black arrows. **b**, AFM photography of the device showing the gold nano-wire over an Al/Al₂O₃ gate. A C_{60} molecule is trapped in the nanogap formed during the electromigration process. **c**, Colour-scale map over two Coulomb diamonds of the differential conductance $\partial I/\partial V$ as a function of bias voltage V_b and gate voltage V_g at 35 mK and zero magnetic field. **d**, Detailed characteristics of the differential conductance in the region “Even”, corresponding to a low bias measurement inside the dotted white rectangle in panel **c**. This region marks the crossing of singlet and triplet spin states of the QD.

transition: i) due to their tunneling geometry, a predominant single screening channel should be expected (similarly to lateral QDs); ii) previous investigations have demonstrated large Kondo temperatures T_K [23, 24, 25] due to the small nanometer size of the QDs molecule; iii) as demonstrated below, gate-tuning of the singlet-triplet gap at zero magnetic field can be obtained and allows the precise tuning of the system across the singlet-triplet boundary. This experiment constitutes an advance in the realization of many-body effects in quantum dots. These results are thus relevant for understanding bulk correlated materials and opens new possibilities for the precise control of spin states in nanostructures containing few electrons.

EXPERIMENTAL SET UP

We briefly discuss the sample preparation and measurement system. A more detailed description details on the measurement is given in the Supplementary Information. We emphasize that the experiment was carried out in a dilution refrigerator with a high degree of filtering, a technical development that was crucial for unveiling the complex quantum phenomena that takes place at low temperatures. Preparation of the single C_{60} transistor was realized by blow drying a dilute toluene solution of the C_{60} molecule onto a gold nano-wire realized on an Al/Al₂O₃ back gate, see Fig. 1b for a schematic view of the setup. Before blow drying the solution, the electrodes were cleaned with acetone, ethanol, isopropanol solution and oxygen plasma. The connected sample is inserted in

a copper shielded box, enclosed in a high frequency low temperature filter, consisting of thermocoax micro-wave filter and Π filters, anchored to the mixing chamber of the dilution fridge having a base temperature equals to 35 mK. The nano-wire coated with molecules is then broken by electromigration [26], via a voltage ramp at 4 K. Our electromigration technique uses real time electronics to monitor the coupling of the single molecule to the electrodes. Here we report a full experimental study of transport measurements on a C_{60} QD, as a function of bias voltage V_b , gate voltage V_g , temperature T (35 mK $< T < 20$ K), and magnetic field B up to 8 T.

OVERVIEW OF TRANSPORT CHARACTERISTICS AT ZERO MAGNETIC FIELD

We start by discussing the general features of the C_{60} QD, on the basis of a large scale two-dimensional map of the differential conductance $\partial I/\partial V$ as a function of both bias V_b and gate V_g voltages, obtained at 35 mK and at zero magnetic field (Fig. 1c). The distinct conducting and non-conducting regions are typical signatures of a single molecule transistor. We present measurements over two distinct Coulomb diamonds indicated by “Odd” and “Even” on Fig. 1c.

In region “Odd”, we measure a sharp high-conductance ridge in the zero-bias $\partial I/\partial V$, which is clearly associated to the usual $S = 1/2$ Kondo effect [4, 25]. This conductance anomaly, connected to the complete quenching of the dot local moment by the conduction electrons, was already investigated at length for other quantum dot systems (see [28] for a review), and we report for comparison in the Supplementary Information a detailed study of the conductance as a function of temperature and magnetic field.

Henceforth we focus on the “Even” Coulomb diamond where an increase in gate voltage results in an additional electron on the dot and thus an even number of total electron. These two-electron states can be described by their total spin S and spin projection m and are noted $|S, m\rangle$. The ground state of the system can thus be either a spin singlet $|0, 0\rangle$ with energy E_S , or a spin triplet with energy E_T described by the three states $\{|1, 1\rangle, |1, 0\rangle, |1, -1\rangle\}$, degenerated at zero magnetic field, but split by the Zeeman effect, with an energy shift $\Delta E_T = mg\mu_B B$ for each state $|1, m\rangle$, where $g \approx 2$ for a C_{60} molecule (See Supplementary Information). Fig. 1d presents a precise low bias $\partial I/\partial V$ measurement of the “Even” region inside the dotted rectangle of Fig. 1c, which clearly displays two distinct regions, which we associate by anticipation to the singlet and triplet ground states respectively. The possibility of a gate-tuning of the singlet-triplet splitting $E_T - E_S$ was demonstrated previously both for lateral quantum dots [14] and carbon nanotube junctions [19].

The two levels cross at a critical gate voltage $V_g^c \simeq 1.9$ V.

In the “Singlet” region, a finite-bias conductance anomaly appears when V_b coincides with $E_T - E_S$, and is explained by a non-equilibrium Kondo effect involving excitations into the spin degenerate triplet. This effect was recently elucidated on a carbon nanotube quantum dot in the singlet state [18]. As shown in the Supplementary Information, our results are consistent with this previous report.

Increasing the gate voltage, and neglecting the electrode coupling which will be discussed in greater details below, the triplet becomes the ground state. Two kinds of resonances are then observed: i) a finite-bias $\partial I/\partial V$ anomaly, interpreted as a singlet-triplet non-equilibrium Kondo effect on the triplet side, that disperses as $E_S - E_T$ in the (V_g, V_b) plane; ii) a sharp zero-bias $\partial I/\partial V$ peak, related to the underscreened spin $S = 1$ Kondo effect [29], as indicated by the low value of the conductance peak.

In order to precisely identify these spin states, and vindicate our later scaling analysis near the singlet-triplet crossing point, we now present a detailed magneto-transport investigation of the “Even” region.

IDENTIFICATION OF THE MAGNETIC STATES IN THE “EVEN” DIAMOND

Due to the high $g \approx 2$ factor of a C_{60} molecule, as compared for instance to $g \approx 0.44$ in GaAs-based devices, it is easier to lift the degeneracy of the triplet state via the Zeeman effect. Figures 2b and 2d show the evolution of the different conductance anomalies in the “Even” Coulomb diamond, as a function of magnetic field.

Fig. 2b shows $\partial I/\partial V$ as a function of the magnetic field up to 8 T, for a constant gate voltage V_g chosen in the “Singlet” region (albeit far from the transition point). In this case, a Zeeman induced transition from the $|0, 0\rangle$ singlet to the lowest $|1, -1\rangle$ triplet occurs by increasing the magnetic field, as sketched in Fig. 2a, and demonstrated by the clear level crossing in the conductance map. The splitting of the threefold triplet is also blatant, and the various spectroscopic lines are consistent with the spin selection rules at both low and high field, where $|0, 0\rangle$ and $|1, -1\rangle$ are the respective ground states.

Fig. 2d investigates the gate-induced singlet-triplet crossing at a constant magnetic field of 3 T. On the singlet side, the Zeeman splitted triplet states are clearly seen as three parallel lines, while the transition lines from the $|1, -1\rangle$ ground state at higher voltage are in agreement with the energy levels depicted in Fig. 2c. Note that due to lower contrast in the “Triplet” region, we have plotted here for better visibility the second order derivative of the current $\partial^2 I/\partial^2 V$.

This gate and magnetic field study gives thus proof of a singlet to triplet transition inside the “Even” diamond. One further remarkable aspect of our data is

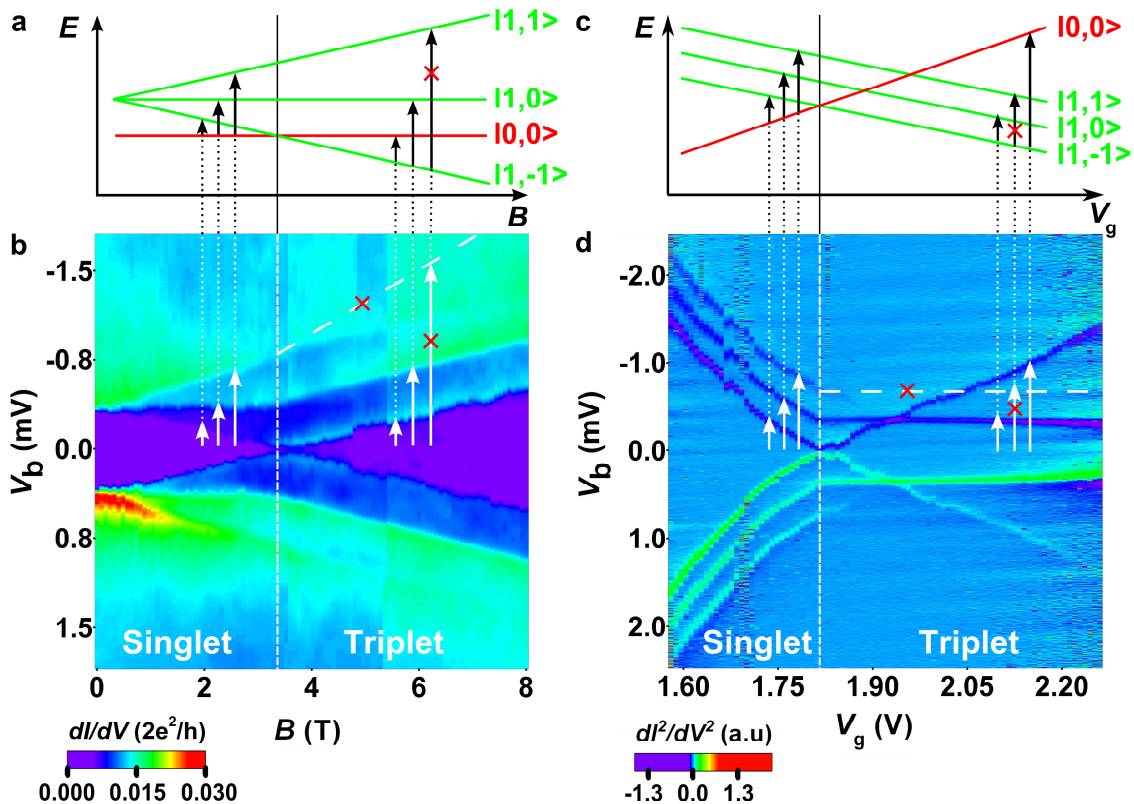


FIG. 2: **Magnetic field and gate induced singlet-triplet transition.** **a**, Schematic of the singlet $|0,0\rangle$ to lowest triplet $|1,-1\rangle$ transition induced by the Zeeman effect. **b**, $\partial I/\partial V$ measurements as a function of B , at fixed gate voltage and temperature $T = 35$ mK. As symbolized by the crossed dotted line and arrow, second order spin flip processes with $\Delta m = 2$ are not observed, see also panel **a**. **c**, Schematic of the singlet $|0,0\rangle$ to lowest triplet $|1,-1\rangle$ transition induced by gate voltage at constant magnetic field. **d**, $\partial^2 I/\partial V^2$ measurements as a function of the gate voltage V_g , at fixed magnetic field $B = 3$ T and temperature $T = 35$ mK.

the absence of a large enhancement of the zero-bias conductance at the singlet-triplet crossing, both in zero-field (Fig. 1d) and in the Zeeman effect (Fig. 2b). Such features were on the contrary observed in previous experiments. In vertical semiconductor quantum dots [11], a field-induced orbital effect can be used to bring the non-degenerate triplet in coincidence with the low-lying singlet state, leading to a spectacular Kondo enhancement of the conductance, which was shown to be associated to two screening channels [30]. In carbon nanotube junctions [16], the Zeeman effect dominates over the orbital effect, so that the transition involves the lowest triplet state only, and Kondo signatures arise from a single channel, which must be however well-balanced between the two orbital states of the quantum dot [31]. The lack of both types of singlet-triplet Kondo effects points towards the predominant coupling between a single screening channel and one of the two spin states of the C_{60} QD, in which case a Kosterlitz-Thouless quantum phase transition should in fact be expected at the singlet-triplet crossing [7, 32].

INVESTIGATION OF THE SINGLET-TRIPLET QUANTUM PHASE TRANSITION

Having established the nature of the magnetic states far from the transition point, we focus now on the conductance for gate voltages V_g close to the critical value V_g^c where singlet and triplet states are brought together at zero magnetic field.

The transition region shown in the middle of Fig. 1d is thus expanded in the conductance map of Fig. 3b taken at the base temperature $T = 35$ mK. We first notice that a sharp conductance dip forms on the singlet side of the transition, in contrast to the shallow minima observed in previous experiments for two-level quantum dots in the singlet regime [14, 19, 20]. Now focusing on the triplet side, we note the presence of two different energy scales (that we will relate to two Kondo screening processes): i) the zero bias peak shows a small and narrowing width, which we connect to a $S = 1$ Kondo temperature $T_{K,1}$; ii) the satellites previously associated to a non-equilibrium singlet-triplet Kondo effect far from the transition point now smoothly merge together to form

a large resonance related to another larger Kondo temperature that we note $T_{K,1/2}$. Both Kondo scales, together with the singlet-triplet splitting, are reported on the schematic phase diagram of Fig. 3a. Several insights on the interpretation in terms of Kondo physics are given by the temperature dependence of the conductance for the different regions labelled.

In region **1** of Fig. 3a we identify two different regimes. Far from the transition point, i.e. when the splitting $E_T - E_S$ exceeds the Kondo temperature $T_{K,1/2}$, the two spins are strongly coupled in a singlet state, and a non-equilibrium Kondo effect involving the degenerate excited triplet state is observed, as previously discussed. The differential conductance exhibits a characteristic U-shape associated with the singlet-triplet gap, as shown by the widest curve in Fig. 5a. Close to the transition point, $E_T - E_S$ can now become smaller than $T_{K,1/2}$, so that the formation of the singlet state involves the hybridization of the conduction electrons. The temperature dependence of the differential conductance in Fig. 4c shows the formation of a narrow dip inside a broader resonance of width $k_B T_{K,1/2}/e$. This dip has been predicted theoretically [7] and here is shown to behave as an inverted Kondo resonance. Specifically, Fig. 4c shows that it has a Lorentzian line shape in bias voltage and Fig. 4d shows its logarithmic temperature dependence at zero bias. More quantitative agreement with the theory can be made by fitting the temperature dependence of the conductance dip with the formula

$$G(T) = G_0 \left[1 - \left(\frac{T^2}{T^{*2}} \left(2^{1/s} - 1 \right) + 1 \right)^{-s} \right] + G_c \quad (1)$$

where the crossover scale T^* is related to the singlet binding energy, G_0 is a typical conductance (both are taken as free parameters), G_c is the background conductance and $s = 0.22$. Taking the experimental value of G_c far from the transition point, good agreement is found with this formula as shown in Fig. 4d. Since the formation of the singlet state is associated with an inverse Kondo effect with a characteristic temperature T^* that depends on the ratio $(E_T - E_S)/T_{K,1/2}$, an universal behavior of the conductance dip is expected near the transition point. Fig. 5a shows that the differential conductance, at the base temperature $T = 35$ mK and for $V_g < V_g^c$, evolves from a Lorentzian to a U-shape, and Fig. 5b shows that this data can be rescaled [33] as a function of $\sqrt{V_b^2 + (k_B T/e)^2}/T^*$. This latter plot shows that the conductance curves collapse on top of each other when taken close to the transition point but that scaling deteriorates as the singlet-triplet gap $E_T - E_S$ becomes greater than $T_{K,1/2}$.

The temperature dependence of $G(T)$ and the V_g -scaling of $\partial I/\partial V$ provide strong evidence that the formation of the spin singlet state near the transition point involves a Kondo process at the low-temperature scale

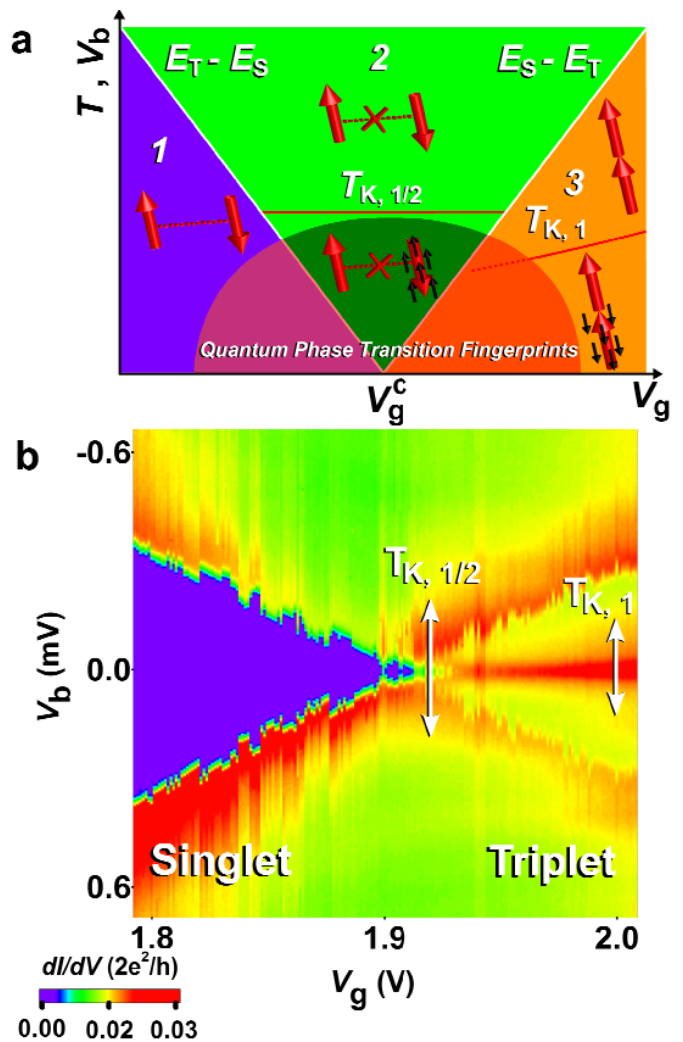


FIG. 3: **Singlet-triplet quantum phase transition.** **a**, Phase diagram as a function of V_g : for simplicity three different regions can be identified depending whether V_b (or T) lies above the singlet-triplet splitting $|E_T - E_S|$. The effective spin states of the QD are represented by large red arrows, and screening electrons by smaller grey arrows. The uncrossed dotted line between the spins signals a strongly bound singlet state in region **1**. In region **2** the two spin states decouple from each other, and the spin which is more strongly coupled to the leads is fully screened via a spin $1/2$ Kondo effect associated to the large Kondo temperature $T_{K,1/2}$. In region **3**, the ground state of the QD is a $S = 1$ triplet, and experiences an incomplete screening associated to the Kondo temperature $T_{K,1}$. **b**, Colour-scale map of the differential conductance $\partial I/\partial V$ as a function of bias V_b and gate V_g voltage at 35 mK and zero magnetic field, close to the singlet to triplet transition, where the scales $|E_T - E_S|$, $T_{K,1/2}$ and $T_{K,1}$ are clearly identified.

T^* , which can be seen as a second stage of screening. The binding of the singlet and its associated conductance dip (inverse Kondo peak) appear inside a much broader resonance of width $T_{K,1/2}$. We argue that this resonance is associated with the spin $S = 1/2$ Kondo effect, the hallmark of the singlet-triplet quantum critical point [7].

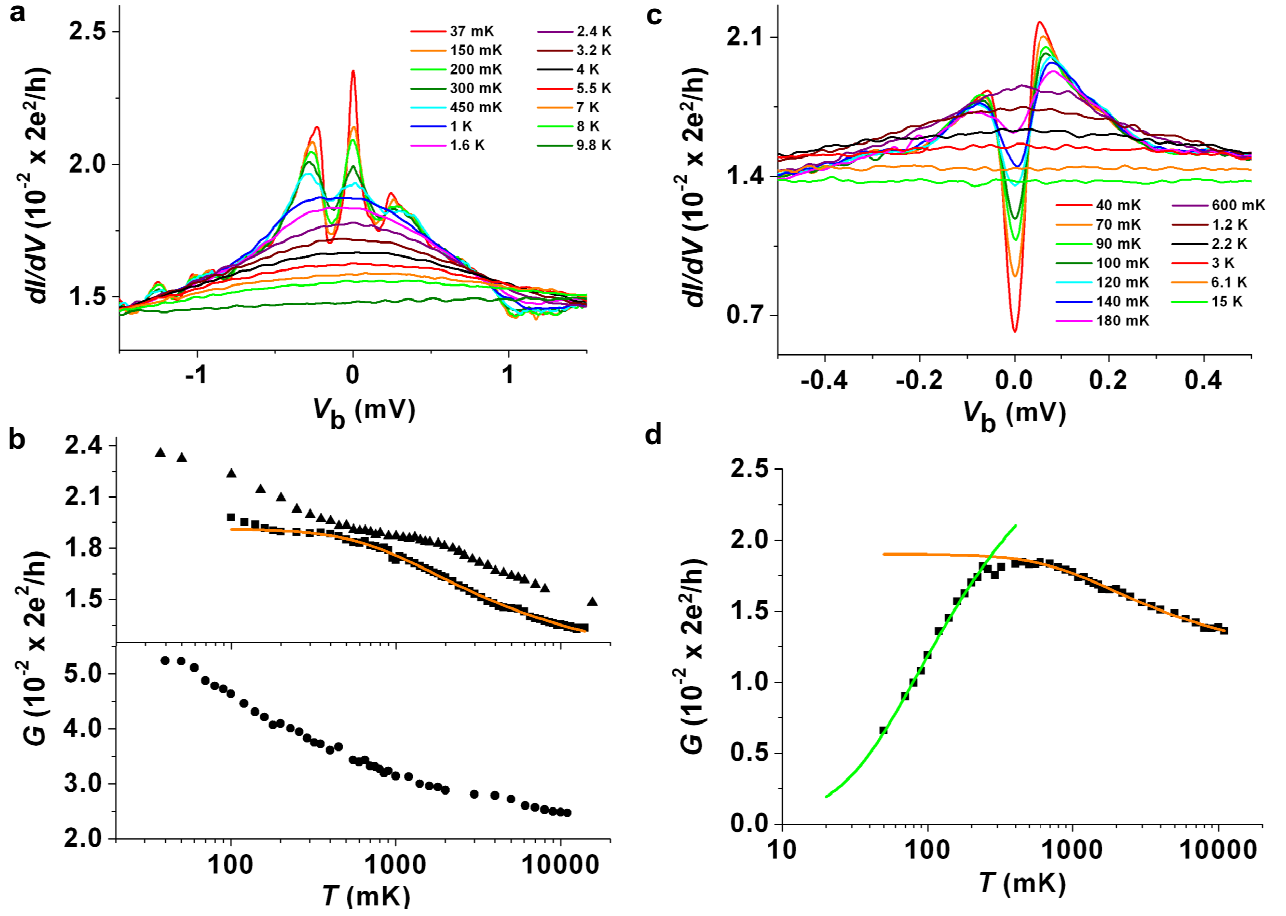


FIG. 4: **Kondo effect in the singlet and triplet state.** **a**, Differential conductance close to the transition point on the triplet side at different temperatures showing a broad resonance with Kondo temperature $T_{K,1/2}$ and Kondo satellites centered at $\pm|E_S - E_T|$. **b**, Temperature dependence of the zero bias conductance $G(T)$ for three gate voltage values in the “Triplet” region, the topmost curve corresponding to the panel **a**. We clearly measure a gate dependent plateau, corresponding to the energy scale $|E_T - E_S|$. The solid line is a fit to Eq. 2 giving $T_{K,1/2} = 3.77$ K. The bottom panel does not show a clear plateau, and correspond to the temperature evolution of $G(T)$ in the underscreen spin $S = 1$ regime. **c**, Differential conductance close to the transition point on the singlet side at different temperatures showing a broad resonance with Kondo temperature $T_{K,1/2}$ and a narrow dip (inverse Kondo effect) associated with a temperature scale T^* . **d**, Temperature dependence of the zero bias conductance $G(T)$ corresponding to the panel **c**. The orange line is a fit to Eq. 2 giving $T_{K,1/2} = 4.13$ K, and the green line is a fit to Eq. 1 giving $T^* = 287$ mK.

To demonstrate this for $T > T^*$ we fit in Fig. 4d $G(T)$ using the formula [27]

$$G(T) = G_0 \left(\frac{T^2}{T_{K,1/2}^2} (2^{1/s} - 1) + 1 \right)^{-s} + G_c \quad (2)$$

where G_0 is the conductance at $T = 0$, G_c is the background conductance, and $s = 0.22$. The good agreement confirms our interpretation of the critical domain (region **2** of Fig. 3a) as a regular spin $S = 1/2$ Kondo effect experienced by one of the two spins. The second spin is disconnected from the leads in this energy range.

We finally turn to the triplet region **3** in Fig. 3a. Far from the transition point, at large gate voltage V_g values, the spins are tightly bound into a triplet and a spin $S = 1$ Kondo effect is expected. Estimates from both the width

of the zero-bias peak and its magnetic field splitting (not shown) converge to a Kondo scale $T_{K,1}$ of the order of 100 mK. This value is unfortunately too low to allow quantitative comparison with theoretical predictions of the underscreened Kondo effect. The conductance $G(T)$ is shown on the lower panel in Fig. 4b, and does not show any sign of saturation down to our effective electronic temperature $T_{\text{eff}} = 50$ mK. When the gate voltage is decreased, a complex regime, where the singlet-triplet splitting $E_S - E_T$ is comparable to the high energy Kondo scale $T_{K,1/2}$, occurs. This is shown by the differential conductance, at fixed V_g with lowering temperature, in Fig. 4a. While a broad peak is again observed at high temperatures, a three-peak structure emerges upon cooling. We interpret the latter by a non-equilibrium Kondo effect that mixes singlet and triplet states via the volt-

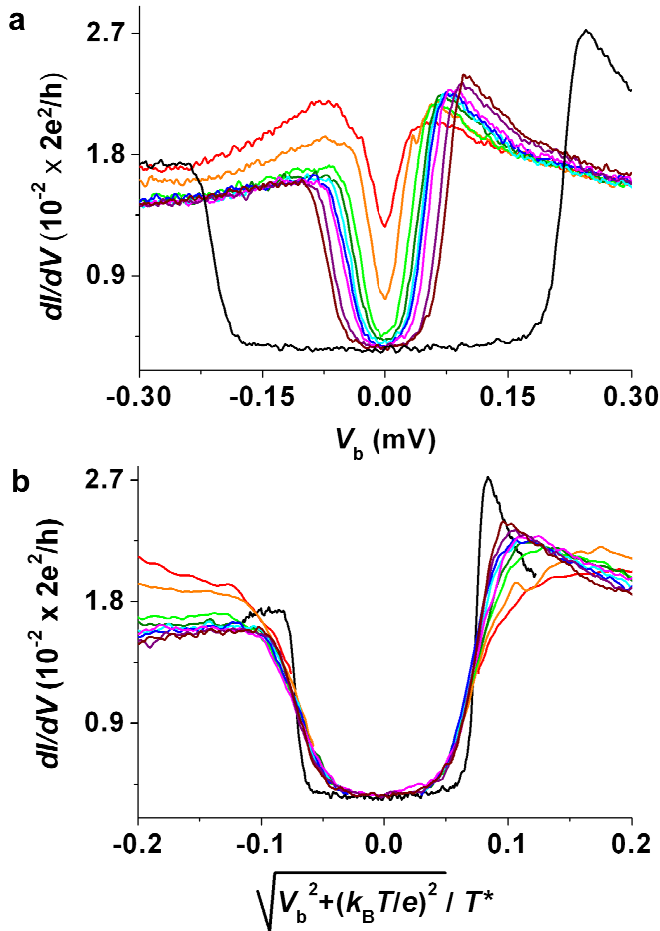


FIG. 5: **Universal scaling.** **a**, Differential conductance for different values of gate voltage $V_g < V_g^c$, close (inverse Kondo effect exhibiting a resonant dip) and far (U-shaped curve) from the transition point. **b**, Scaling analysis of the data of panel **a**, with respect to the singlet binding energy T^* .

age bias window. We associate the former with a spin $S = 1/2$ Kondo effect, similarly to what occurs on the singlet side. This idea is consistent with the corresponding zero-bias conductance $G(T)$ for temperatures above the singlet-triplet splitting, as shown by the upper panel in Fig. 4b. The spin $S = 1/2$ Kondo behavior of $G(T)$ extend down to the lowest temperatures by approaching the critical point, as $E_S - E_T$ becomes smaller than $T_{K,1/2}$. This is most clearly displayed by the lower curve of the same plot, to which a fit with equation (2) can be successfully performed. The further increase of $G(T)$ below 200mK is at present not fully understood, and may be related to the opening of a second screening channel, which would possibly spoil the quantum critical point at zero temperature [34]. However, this extra feature seems related to a very small energy scale close to the crossing point, so that the interpretation of the data in the acces-

sible temperature range is consistent with the quantum critical point scenario. We finally note that our data can be analyzed in a complementary way (given in the Supplementary Information) by plotting the zero-bias conductance as a function of gate voltage, for different temperatures. By cooling, this shows the clear sharpening of a conductance step when the system crosses from singlet to triplet, in agreement with the existence of a quantum critical point [7], and in contrast to the maximum predicted for an avoided transition [30, 34].

We end by noting that the singlet-triplet transition in a C_{60} molecular junction differs fundamentally from the observations in semiconductor [11] and nanotube [16] dots, thus showing the potentiality of combining well-controlled electromigration techniques with molecules of complex chemistry.

Acknowledgments We gratefully acknowledge E. Eyraud, D. Lepoittevin for their useful electronic and dilution technical contributions and motivating discussions. We thank E. Bonet, T. Crozes and T. Fournier for lithography development, C. Winkelmann, T. Costi and L. Calvet for invaluable discussions. The sample of the investigations was fabricated in the NANOFAB facility of the Néel Institut. This work is partially financed by ANR-PNANO Contract MolSpintronics No. ANR-06-NANO-27.

-
- [1] Sachdev, S. Quantum Phase Transitions. *Cambridge University Press*, Cambridge (1999).
 - [2] Hewson, A. C. The Kondo Problem to Heavy Fermions. *Cambridge University Press*, Cambridge (1993).
 - [3] Glazman, L. I. & Raikh, M. E. Resonant Kondo transparency of a barrier with quasilocal impurity states. *JETP Lett.* **47**, 452, (1988).
 - [4] Goldhaber-Gordon, D. *et al.* Kondo effect in a single-electron transistor. *Nature* **391**, 156-159 (1998).
 - [5] Cronenwett, S. M., Oosterkamp, T. H. & Kouwenhoven, L. P. A Tunable Kondo Effect in Quantum Dots. *Science* **281**, 540-544 (1998).
 - [6] Vojta, M., Bulla, R. & Hofstetter, W. Quantum phase transitions in models of coupled magnetic impurities. *Phys. Rev. B* **65**, 140405 (2002).
 - [7] Hofstetter, W. & Schoeller, H. Quantum Phase Transition in a Multilevel Dot. *Phys. Rev. Lett.* **88**, 016803 (2002).
 - [8] Georges, A. & Meir, Y. Electronic Correlations in Transport through Coupled Quantum Dots. *Phys. Rev. Lett.* **82**, 3508 (1999).
 - [9] Jones, B. A., Varma, C. M. & Wilkins, J. W. Low-Temperature Properties of the Two-Impurity Kondo Hamiltonian. *Phys. Rev. Lett.* **61**, 125-128 (1988).
 - [10] Löhneysen, H.v., Rosch, A., Vojta, M. & Woelfle, P. Fermi-liquid instabilities at magnetic quantum phase transitions. *Rev. Mod. Phys.* **79**, 1015-1075 (2007).
 - [11] Sasaki, S. *et al.* Kondo effect in an integer-spin quantum dot. *Nature* **405**, 764-767 (2000).
 - [12] Schmid, J., Weis, J., Eberl, K. & Klitzing, K. v. Absence

- of Odd-Even Parity Behavior for Kondo Resonances in Quantum Dots. *Phys. Rev. Lett.* **84**, 5824-5827 (2000).
- [13] van der Wiel, W. G. *et al.*. Two-Stage Kondo Effect in a Quantum Dot at a High Magnetic Field. *Phys. Rev. Lett.* **88**, 126803 (2002).
- [14] Kogan, A., Granger, G., Kastner, M. A., Goldhaber-Gordon, D. & Shtrikman, H. Singlet-triplet transition in a single-electron transistor at zero magnetic field. *Phys. Rev. B* **67**, 113309 (2003).
- [15] Vidan, A., Stopa, M., Westervelt, R. M., Hanson, M. & Gossard, A. C. Multipeak kondo Effect in One- and Two-Electron Quantum Dots. *Phys. Rev. Lett.* **96**, 156802 (2006).
- [16] Nygård, J., Cobden, D. H. & Lindelof, P. E. Kondo physics in carbon nanotubes. *Nature* **408**, 342-346 (2000).
- [17] Jarillo-Herrero, P. *et al.*. Electronic Transport Spectroscopy of Carbon Nanotubes in a Magnetic Field. *Phys. Rev. Lett.* **94**, 156802 (2005).
- [18] Paaske, J. *et al.*. Non-equilibrium singlet-triplet Kondo effect in carbon nanotubes. *Nature Physics* **2**, 460-464 (2006).
- [19] Quay, C. H. L. *et al.* Kondo Physics in Nanotubes: Magnetic-field dependence and singlet-triplet Kondo. *cond. mat.*, <http://arxiv.org/pdf/0704.3641> (2007).
- [20] Craig, N.J. *et al.* Tunable Nonlocal Spin Control in a Coupled-Quantum Dot System. *Science* **304**, 565-567 (2004).
- [21] Affleck, I., Ludwig, A. W. W. & Jones, B. A. Conformal-field-theory approach to the two-impurity kondo problem: Comparison with numerical renormalization-group results. *Phys. Rev. B* **52**, 9528-9546, (1995).
- [22] Zarand, G., Chung, C.-H., Simon, P. & Vojta, M. Quantum Criticality in a Double-Quantum-Dot System. *Phys. Rev. Lett.* **97**, 166802 (2006).
- [23] Liang, W., Shores, M. P., Bockrath, M., Long, J. R. & Park, H. Kondo resonance in a single-molecule transistor. *Nature* **417**, 725-729 (2002).
- [24] Park, J. *et al.*. Coulomb blockade and the Kondo effect in single-atom transistor. *Nature* **417**, 722-725 (2002).
- [25] Yu, L. H. & Natelson, D. The Kondo Effect in C₆₀ Single-Molecule Transistors. *Nano Lett.* **4**, 79-83 (2004).
- [26] Park, H., Lim, A. K. L., Alivisatos, A. P., Park, J. & McEuen, P. L.. Fabrication of metallic electrodes with nanometer separation by electromigration. *Appl. Phys. Lett.* **75**, 301-303 (1999).
- [27] Goldhaber-Gordon, D. *et al.*. From the Kondo regime to the Mixed-Valence Regime in a Single-Electron Transistor. *Phys. Rev. Lett.* **81**, 5225-5228 (1998).
- [28] Grobis, M., Rau I. G., Potok, R. M. & Goldhaber-Gordon, D. Kondo Effect in Mesoscopic Quantum Dots. *Handbook of Magnetism and Magnetic Materials*, Kronmüller, H. & Parkin, S. eds. Wiley (2007).
- [29] Nozières, P. & Blandin, A. Kondo effect in real metals. *J. Phys. (Paris)* **41**, 193 (1980).
- [30] Pustilnik, M. & Glazman, L. I. Kondo effect induced by a magnetic field. *Phys. Rev. B* **64**, 045328 (2001).
- [31] Pustilnik, M., Avishai, Y. & Kikoin, K. Quantum dot with even number of electrons: Kondo effect in a finite magnetic field. *Phys. Rev. Lett.* **84**, 1756 (2000).
- [32] Cornaglia, P. S. & Grepel, D. R. Strongly correlated regimes in a double quantum dot device. *Phys. Rev. B* **71**, 075305 (2005).
- [33] Potok, R. M., Rau, I. G., Shtrikman, H., Oreg, Y. & Goldhaber-Gordon, D. Observation of the two-channel Kondo effect. *Nature* **446**, 167-171 (2006).
- [34] Hofstetter, W. & Zarand, G. Singlet-triplet transition in lateral quantum dots: A numerical renormalization group study. *Phys. Rev. B* **69**, 235301 (2004).